NASA
Technical Memorandum 81446

AVRADCOM
Technical Report 80-C-5

IDEAL SPIRAL BEVEL GEARS - A NEW APPROACH TO SURFACE GEOMETRY

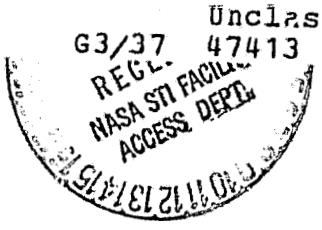

R. L. Huston
University of Cincinnati
Cincinnati, Ohio

and

J. J. Coy
Propulsion Laboratory
AVRADCOM Research and Technology Laboratories
Lewis Research Center
Cleveland, Ohio

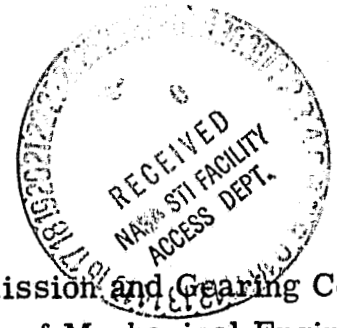

Prepared for the
Third International Power Transmission and Gearing Conference
sponsored by the American Society of Mechanical Engineers
San Francisco, California, August 18-22, 1980

IDEAL SPIRAL BEVEL GEARS - A NEW APPROACH TO SURFACE GEOMETRY

by R. L. Huston*
University of Cincinnati
Cincinnati, Ohio

and

J. J. Coy*
Propulsion Laboratory
AVRADCOM Research and Technology Laboratories
Lewis Research Center
Cleveland, Ohio

ABSTRACT

This paper discusses the fundamental geometrical characteristics of spiral bevel gear tooth surfaces. The parametric representation of an ideal spiral bevel tooth is developed. The development is based on the elements of involute geometry, differential geometry, and fundamental gearing kinematics. A foundation is provided for the study of nonideal gears and the effects of deviations from ideal geometry on the contact stresses, lubrication, wear, fatigue life, and gearing kinematics.

E-366

NOTATION

A,A'	points on a circular disk (Figs. 2 to 4)
a	logarithmic spiral constant
B,B'	points on a circular disk (Fig. 4)
$\underset{\sim}{b}$	position vector to a typical point on the gear tooth surface
C	involute generating circle (Fig. 1)
det g_{ij}	determinant of g_{ij}
$\underset{\sim}{e}_i$ (i=1,2)	base vectors tangent to the gear tooth surface
g	det g_{ij}

*Member ASME.

g_{ij} (i,j=1,2)	gear tooth surface metric tensor
g^{-1}_{ij} (i,j=1,2)	inverse tensor of g_{ij}
h	det h_{ij}
h_i (i=1,2)	surface fundamental vectors (Eq. (12))
h_{ij} (i,j=1,2)	second fundamental tensor (Eq. (13))
I	involute curve (Figs. 1 and 6)
J	mean curvature
K	Gaussian curvature
m	logarithmic spiral constant
$\underset{\sim}{N}_1, \underset{\sim}{N}_2, \underset{\sim}{N}_3$	mutually perpendicular unit vectors (Figs. 6, 7, and 9)
$\underset{\sim}{N}'_1, \underset{\sim}{N}'_2, \underset{\sim}{N}'_3$	mutually perpendicular unit vectors (Figs. 7 to 9)
$\underset{\sim}{N}_4$	a unit vector parallel to OP (Fig. 9)
$\underset{\sim}{n}$	a unit vector normal to the gear tooth surface
O	disk center (Figs. 2 and 4) and base cone apex (Figs. 6 to 8)
O'	center of involute generating circle (Fig. 1) and back cone apex (Figs. 6, 8, and 9)
$\hat{O}$	center of base cone/back cone intersection circle (Figs. 2, 6, and 9)
P	a typical point on an involute curve (Fig. 1) and the gear tooth surface
P'	point of intersection of line segment O'P and the base cone/back cone intersection (Figs. 1 and 9)
Q	base point of involute curve (Fig. 1) and typical point on the base cone/gear tooth intersection (Figs. 6 to 9)

R	involute circle radius (Fig. 1) and back cone element length (Figs. 6 and 8)
R_{max}, R_{min}	maximum and minimum gear tooth surface radii of curvature
r	disk radius (Fig. 2) and base cone element distance (Figs. 3, 6, 8)
r_0	radius of base cone/back cone intersection circle (Fig. 2)
S	a general surface
T	tangent to involute generating circle (Fig. 1)
u^1, u^2	surface parameters
x	length of line segment O'P (Fig. 1)
α	base cone half central angle (Figs. 2, 3, 6, and 8)
α_c	back cone half central angle (Figs. 6, 8, and 9)
β	involute generating angle (Fig. 1)
γ	complement to the spiral angle (Fig. 5)
δ	cut out sector angle (Fig. 2)
φ	involute generating angle (Fig. 1) and central disk angle (Fig. 4)
$\hat{\varphi}$	central angle in the base of a cone from a spindled disk (Fig. 4) and involute angle in the base-cone/back-cone intersection (Fig. 9)
ψ	spiral angle (Fig. 5)
ϑ	polar angle
$\hat{\vartheta}$	projected polar angle (Figs. 7 and 9)

INTRODUCTION

Recently, there has been renewed interest in the efficiency, reliability, and life of gearing and power transmission systems - particularly those used in helicopters and other aircraft. This interest is due in part to the recent concern about quality control and the safety of aircraft parts together with an increased emphasis on energy conservation. Beyond this, however, there is a continual interest in understanding the basic phenomena of lubrication, surface fatigue, and wear which directly affect the reliability, life and efficiency of mechanical components in transmission systems. Of particular interest is the role of spiral bevel gear tooth surface geometry and how it affects the performance and life of the transmission.

The geometrical characteristics and parameters of spiral gears have been documented for some time by the American Gear Manufacturer's Association and others [1-11].** However, most of this documentation is not immediately applicable as an analytical basis for using some of the modern approaches to surface geometry - particularly, computer analyses which could be very helpful in studying these widely used gears. Also, much of the documentation on spiral bevel gears pertains to circular-cut as opposed to true-spiral-cut gears. Therefore, the objective of this paper, is to provide an exposition on a fundamental approach and analysis of the spiral bevel gear surface geometry. The emphasis is upon characterizing the geometry so that the fundamental quantities and relations such as surface parametric equations, radii of curvature and meshing kinematics can be systematically determined.

**Numbers in brackets refer to references at the end of the paper.

The balance of the paper is divided into four sections with the following section providing some preliminary background concepts which will be useful in the sequel. The next section is a description of the ideal spiral bevel gear tooth itself. This is followed by a detailed analytical description of the surface geometry of this ideal gear. The final section presents a discussion of the application and potential for further development of the analysis.

PRELIMINARY CONSIDERATIONS

Involute Geometry

Spiral bevel gears (and also hypoid gears) could be considered to be at the top of a hierarchy of gears beginning with spur gears and then to helical gears, then to straight bevel gears and skewed bevel gears, and finally to spiral bevel gears. In each of these gears a tooth geometry can be developed by generalizing the involute geometry commonly associated with spur gears. Therefore, for notational and other purposes it will be helpful to briefly restate some of the fundamentals of involute curve geometry.

Consider the involute curve I, shown in Fig. 1, which for simplicity may be considered as the curve traced by the end of a cord being unwrapped around the circle C. O' is the center of C and P is a typical point on I. Q is at the base of I. The line segments QO' and PO' then form an angle φ as shown. T is the tangent point of the tangential segment PT. The segments TO' and QO' then form the angle β. Finally, P' is the intersection point of O'P and C.

If R is the circle radius, it is immediately seen that the radius of curvature ρ of I at P is

$$\rho = R\beta \tag{1}$$

Hence, in terms of β, it is easily seen that

$$x = R(1 + \beta^2)^{1/2} \tag{2}$$

and that

$$\varphi = \beta - \tan^{-1}\beta \tag{3}$$

where x is the length of the line segment $O'P$. (Eq. (2) follows immediately Eq. (1) and the Pythagorean identity and Eq. (3) is obtained by observing that $\tan(\beta - \varphi) = \rho/R$.)

Spindling a Disk into a Cone

Just as a spur gear can be generated by "wrapping" a basic rack into a circle, so also a bevel gear can be generated by spindling a "crown gear" (a circular disk or face gear, sometimes called a "crown rack") into a cone. Therefore, it is useful to review the geometrical aspects of spindling a disk into a cone.

Consider the disk with radius r with a cut-out sector with angle δ as shown in Fig. 2. If points A and A' are brought together, the disk forms a cone as shown in Fig. 3. Letting r_0 be the radius at the base of the cone, it is immediately seen that

$$2\pi r_0 = (2\pi - \delta)r \tag{4}$$

Therefore, if α is the half central angle of the cone, α and δ are related as

$$\sin\alpha = r_0/r = 1 - (\delta/2\pi) \tag{5}$$

Finally, consider the disk of Fig. 2 with two points B and B' on the circumference. Then B and B' with O form the angle φ as shown in Fig. 4(a). After spindling, the top view of the resulting cone is shown in Fig. 4(b), where $\hat{O}$ is on the cone axis at its base. Since the ares BB' are of equal lengths in Figs. 4(a) and (b), the angle $\hat{\varphi}$ formed by B, $\hat{O}$, and B' is then related to φ through the equation

$$r\varphi = r_0\hat{\varphi} \tag{6}$$

or, by using Eq. (5) as

$$\hat{\varphi} = \varphi/\sin\alpha \tag{7}$$

Differential Geometry Formulation

Major factors affecting the lubrication, surface fatigue, contact stress, wear, and life of gear teeth are the maximum and minimum radii of curvature of the tooth surface at the point of contact with the meshing tooth. To obtain the radii of curvature, it is convenient to employ some relations developed in elementary differential geometry formulations. Hence, these relations are briefly summarized here.

Suppose a surface S is described by a pair of parameters u_1 and u_2 through the vector parametric equation $\underset{\sim}{p} = \underset{\sim}{p}(u_1,u_2)$ where $\underset{\sim}{p}$ is the position vector of a typical point P on S. Then base vectors $\underset{\sim}{e}_i$ (i = 1,2) tangent to S at P are given by

$$\underset{\sim}{e}_i = \partial p/\partial u^i \quad (i = 1,2) \tag{8}$$

A surface metric tensor g_{ij} (i,j = 1,2) may then be defined as

$$g_{ij} = \underset{\sim}{e}_i \cdot \underset{\sim}{e}_j \quad (i = 1,2) \tag{9}$$

Let g be det g_{ij}. Then it is easily shown that

$$g = |\underset{\sim}{e}_1 \times \underset{\sim}{e}_2| \tag{10}$$

Hence, a unit vector $\underset{\sim}{n}$ normal to S is given by

$$\underset{\sim}{n} = \underset{\sim}{e}_1 \times \underset{\sim}{e}_2 / g \tag{11}$$

Next, let the fundamental vectors $\underset{\sim}{h}_i$ $(i = 1,2)$ be defined as

$$\underset{\sim}{h}_i = -\underset{\sim}{n}/u^i \quad (i = 1,2) \tag{12}$$

Then the second fundamental tensor h_{ij} $(i,j = 1,2)$ is defined as

$$h_{ij} = -\underset{\sim}{h}_i \cdot \underset{\sim}{e}_j \quad (i,j = 1,2) \tag{13}$$

Finally, the Gaussian curvature K and the mean curvature J are defined as

$$K = h/g \tag{14}$$

and

$$J = k_{ii} \tag{15}$$

where h is $\det h_{ij}$ and k_{ij} is defined as

$$k_{ij} = g^{-1}_{ir} h_{rj} \tag{16}$$

where g^{-1}_{ij} is the inverse tensor of g_{ij}. Regarding notation, repeated indices represent a sum (that is, from 1 to 2) over that index.

The maximum and minimum radii of curvature R_{max} and R_{min} are then easily calculated in terms of J and K as

$$R_{max}, R_{min} = 2/J \pm (J^2 - 4K)^{1/2} \tag{17}$$

AN IDEAL SPIRAL BEVEL GEAR TOOTH SURFACE GEOMETRY

A Logarithmic Spiral

The name "spiral-bevel" stems from the fact that if the centerline of a crown gear tooth follows a logarithmetic spiral, the spiral angle will be constant along the tooth. That is, the tangent to the tooth centerline makes a constant angle with the radial lines. Figure 5 illustrates this

where ψ_1 and ψ_2 are the angles between the tooth centerline and the radial lines at typical points P_1 and P_2. It is easily shown [12] that if the polar form of the tooth centerline equation is $r = ae^{m\theta}$, a logarithmic spiral, then $\psi_1 = \psi_2$. That is, the spiral angle is constant along the tooth. This is significant since then the complementary angles γ_1 and γ_2 are also equal and therefore constant along the tooth. This means that the tooth profile, which is normal to the radial direction, makes a constant angle with the tooth centerline. This, in turn, is significant since it insures uniform meshing kinematics along the gear tooth with the mating gear.

The following subsection examines the spindling of a crown gear, with gear teeth in the shape of logarithmetic spirals, into a cone.

Base Cone Geometry

To develop the geometrical basis of an ideal spiral bevel gear, imagine a crown gear with an involute tooth profile. (The tooth profile is normal to the radial direction.) Next, let this gear be spindled into a cone as described in the foregoing section. The details of this can be seen by considering Fig. 6 where the "base cone" and a corresponding orthogonal "back cone" of a typical gear are shown. In this figure, Q is a typical point on the base cone of a gear tooth. R is the elemental distance from the back cone apex O' to the base-cone/back-cone intersection. Similarly, r is the elemental distance from the base cone apex to the base-cone/back-cone intersection. α and α_c are the half central angles of the base and back cones respectively. (α_c is the complement of α.) $\underset{\sim}{N}_1$, $\underset{\sim}{N}_2$, and $\underset{\sim}{N}_3$ are mutually perpendicular unit vectors with $\underset{\sim}{N}_3$ being parallel to the cone axis. Figure 6 also shows an exaggerated view

of an involute curve I starting at Q and being wrapped around the base cone. Here, as in Fig. 1, R corresponds to the radius of the circle of the unwrapping cord which defines the involute. That is, the curve is formed by unwrapping a cord about a circle of radius R and then by spindling the resulting involute around the back cone. Finally, in Fig. 6, $\underset{\sim}{OQ}$ is the position vector of Q relative to O and its magnitude is r.

Figure 7 shows a top view of the base-cone/back-cone intersection of Fig. 6. $\hat{\vartheta}$ is the angle between $\underset{\sim}{N}_1$ and the projection of $\underset{\sim}{OQ}$ onto the intersection plane. $\underset{\sim}{N}'_1$, $\underset{\sim}{N}'_2$, and $\underset{\sim}{N}'_3$ are mutually perpendicular unit vectors with $\underset{\sim}{N}'_3$ coinciding with $\underset{\sim}{N}_3$. Figure 7 also shows the logarithmic spiral spindled about the base cone. If the logarithmic spiral is defined by $r = ae^{m\vartheta}$ as described in the preceding subsection, then $\hat{\vartheta}$ is related to ϑ by Eq. (7). That is,

$$\hat{\vartheta} = \vartheta/\sin\alpha \tag{18}$$

Position Vectors

The surface geometry of a spiral bevel gear tooth is determined once a position vector to a typical point P on the tooth surface is known. Relative to O, the base cone apex, such a position vector could take the form

$$\underset{\sim}{P} = \underset{\sim}{OP} = \underset{\sim}{OQ} + \underset{\sim}{QQ'} + \underset{\sim}{Q'P} \tag{19}$$

where the notation is self-defining. By examining Figs. 6 and 7, it is readily seen that in terms of $\underset{\sim}{N}_1$, $\underset{\sim}{N}_2$, and $\underset{\sim}{N}_3$, $\underset{\sim}{OQ}$ is:

$$\underset{\sim}{OQ} = r\sin\alpha\cos\hat{\vartheta}\,\underset{\sim}{N}_1 + r\sin\alpha\sin\hat{\vartheta}\,\underset{\sim}{N}_2 - r\cos\alpha\,\underset{\sim}{N}_3 \tag{20}$$

Next, consider Fig. 8 which shows a true view of the vectors $\underset{\sim}{OQ}$ and $\underset{\sim}{QQ'}$. From this figure, it is immediately seen that R is equal to $r\tan\alpha$ and that $\underset{\sim}{QQ'}$ is then given by

$$O'P = r \tan \alpha \cos \alpha N_1' + r \tan \alpha \sin \alpha N_2' \qquad (21)$$

Finally, to determine $O'P$, note that from Fig. 1, $O'P$ can be written in the simple form

$$O'P = x N_3 \qquad (22)$$

where x is given by Eq. (2) and where N_3 is a unit vector parallel to $O'P$ as shown in Fig. 9. If N_1'' is a unit vector parallel to OP' as shown, N_3 may be written as

$$N_3 = \sin \alpha_c N_1'' + \cos \alpha_c N_3 \qquad (23)$$

However, N_1'' may be expressed in terms of N_1 and N_2 as

$$N_1'' = \cos(\hat{\theta} + \hat{\gamma}) N_1 + \sin(\hat{\theta} + \hat{\gamma}) N_2 \qquad (24)$$

where $\hat{\gamma}$ is projected involute generating angle. $\hat{\gamma}$ is related to γ of Fig. 1, by Eq. (7). That is,

$$\hat{\gamma} = \gamma / \sin \alpha_c \qquad (25)$$

Hence, from Eqs. (22) to (24) $O'P$ becomes

$$O'P = x \sin \alpha_c \cos(\hat{\theta} + \hat{\gamma}) N_1 + x \sin \alpha_c \sin(\hat{\theta} + \hat{\gamma}) N_2 + x \cos \alpha_c N_3 \qquad (26)$$

Finally, by using Eqs. (19), (20), (21), and (26), P_c becomes

$$P_c = x \sin \alpha_c \cos(\hat{\theta} + \hat{\gamma}) N_1 + x \sin \alpha_c \sin(\hat{\theta} + \hat{\gamma}) N_2 + (x \cos \alpha_c - r \sec \alpha) N_3 \qquad (27)$$

By noting that α and α_c are complementary (hence, $\sin \alpha_c = \cos \alpha$ and $\cos \alpha_c = \sin \alpha$) and that by Eq. (2) $x = r(1 + \hat{\gamma}^2)^{1/2} \tan \alpha$, Eq. (27) may be rewritten as

$$P_c = r (1 + \hat{\gamma}^2)^{1/2} \sin \alpha \cos(\hat{\theta} + \hat{\gamma}) N_1 + (1 + \hat{\gamma}^2)^{1/2} \sin \alpha \sin(\hat{\theta} + \hat{\gamma}) N_2 + (1 + \hat{\gamma}^2)^{1/2} \sin \alpha \tan \alpha - \sec \alpha N_3 \qquad (28)$$

Equation (28) can be shown to be of the form $p = p(u^1,u^2)$ where $u^1 = \hat{\vartheta}$ and $u^2 = \lambda$. This is immediately seen by recalling from Eqs. (4) and (7) that r and $\hat{\phi}$ may be written as

$$r = a \exp(m \hat{\vartheta} \sin \alpha) \tag{29}$$

and

$$\hat{\phi} = (\lambda - \tan^{-1}\lambda)/\cos \alpha \tag{30}$$

Differential Geometry

If Eq. (28) is considered to be of the form $p = p(\hat{\vartheta},\lambda) = p(u^1,u^2)$, then the differential geometry formulas of Eqs. (8) to (17) are directly applicable. For example, it is easily shown that the base vectors and metric tensor components are:

$$\begin{aligned} e_1 = {} & r(1+\lambda^2)^{1/2} \sin\alpha\,[m \sin\alpha \cos(\hat{\theta}+\hat{\phi}) - \sin(\hat{\theta}+\hat{\phi})]N_1 \\ & + r(1+\lambda^2)^{1/2} \sin\alpha\,[m \sin\alpha \sin(\hat{\theta}+\hat{\phi}) + \cos(\hat{\theta}+\hat{\phi})]N_2 \\ & + m\, r \tan\alpha\,(1+\lambda^2)^{1/2}(\sin^2\alpha - 1)N_3 \end{aligned} \tag{31}$$

$$\begin{aligned} e_2 = {} & r\lambda(1+\lambda^2)^{1/2} \sin\alpha\,[\cos(\hat{\theta}+\hat{\phi}) - \lambda \sin(\hat{\theta}+\hat{\phi})\sec\alpha]N_1 \\ & + [\sin(\hat{\theta}+\hat{\phi}) + \lambda \cos(\hat{\theta}+\hat{\phi})\sec\alpha]N_2 + (\tan\alpha)N_3 \end{aligned} \tag{32}$$

$$\begin{aligned} g_{11} = {} & r^2(1+\lambda^2)\sin^2\alpha(m^2\sin^2\alpha + 1) \\ & + m^2 r^2 \tan^2\alpha\,(1+\lambda^2)^{1/2}(\sin^2\alpha - 1)^2 \end{aligned} \tag{33}$$

$$g_{12} = g_{21} = r^2\lambda \sin\alpha\,[m\lambda + m \tan\alpha - m(1+\lambda^2)^{1/2}\tan\alpha] \tag{34}$$

and

$$g_{22} = r^2\lambda^2\tan^2\alpha \tag{35}$$

Beyond this however, a glance at Eqs. (11), (12), (16), and (17) shows that calculation of the unit normal vector, the second fundamental tensor, and the radii of curvature, could be quite laborious and cumbersome. Hence, they are not presented here. However, the expressions of Eqs. (11) to (17) are in ideal form for calculation by one of the symbolic manipulative computer languages (e.g., FORMAC).

SUMMARY OF RESULTS AND CONCLUSIONS

The foregoing is a brief exposition and analysis of the fundamental geometrical characteristics of an ideal spiral bevel gear. The basis of the exposition is the assumption of a gear tooth having an involute profile and a centerline which follows a logarithmic spiral. Although such gears may not be convenient to manufacture and machine, a few conclusions about them and "nonideal" gears may be immediately deduced: First, it is clear that unless the tooth centerline follows a logarithmic spiral, the inclination of the tooth profile, which engages the meshing gear, will not be uniform along the tooth. This could adversely modify the surface characteristics which in turn could affect the contact stress, lubrication, and wear of the gear. Next, if a true involute profile is not employed, conjugate action of involute gearing could be affected, thus inducing vibrations and erratic kinematics. Finally, unless the gear tooth is spindled around the base cone, there could occur excessive sliding at the heel and toe of the tooth during meshing - particularly if the tooth is long and is developed by a plane (e.g., circular) cutter.

Beyond this however, the foregoing analysis can provide a basis for the analysis and comparison of nonideal gears and for estimating the

significance of deviations from an ideal form. Moreover, the analysis is developed in a form that is suited for modern computer analyses and symbolic manipulator languages.

ACKNOWLEDGEMENT

The work reported herein was partially funded under NASA Lewis Research Center grant NSG 3188 with the University of Cincinnati.

REFERENCES

1. "AGMA Standard Gear Nomenclature - Terms, Definitions, Symbols and Abbreviations," AGMA Publication 112.05, 1976.

2. "AGMA Reference Information - Basic Gear Geometry," AGMA Publication 115.01, 1959.

3. "AGMA Standard System for Spiral Bevel Gears," AGMA Publication 209.03, 1964.

4. Buckingham, E., Analytical Mechanics of Gears, Dover, New York, 1963.

5. Dyson, A., A General Theory of the Kinematics and Geometry of Gears in Three Dimensions, Clarendon Press, Oxford, 1969.

6. Baxter, M. L., Jr., "Exact Determination of Tooth Surfaces for Spiral Bevel and Hypoid Gears," AGMA Semi-Annual Meeting, American Gear Manufacturers Association, 1966, Paper No. 139.02.

7. Coleman, W., "Guide to Bevel Gears," Product Engineering, Vol. 34, June 10, 1963, p. 87.

8. Coleman, W., "Effect of Mounting Displacements on Bevel and Hypoid Gear Tooth Strength," SAE Paper No. 750151, Feb. 1975.

9. Krenzer, T. J., "The Effect of Cutter Radius on Spiral Bevel and Hypoid Tooth Contact Behavior," AGMA Semi-Annual Meeting, American Gear Manufacturers Association, 1976, Paper No. 129.21.

10. Bonsignore, A. T., "The Effect of Cutter Diameter on Spiral Bevel Tooth Proportions," AGMA Semi-Annual Meeting, American Gear Manufacturers Association, 1976, Paper No. 124.20.

11. Litvin, F. L., "Relationships Between the Curvatures of Tooth Surfaces in Three-Dimensional Gear Systems," NASA TM X-75130, 1977.

12. Schwartz, A., Analytic Geometry and Calculus, Holt, Rinehart, and Winston, New York, 1960, p. 528.

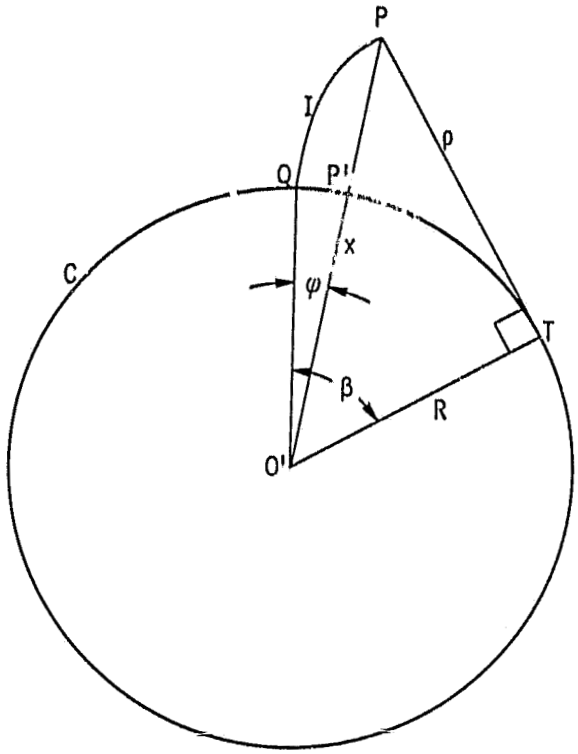

Figure 1. - Involute geometry.

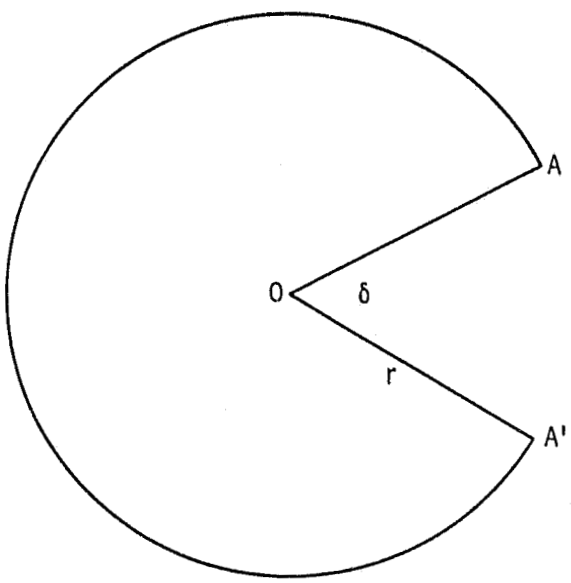

Figure 2. - Circular disk with cut out sector.

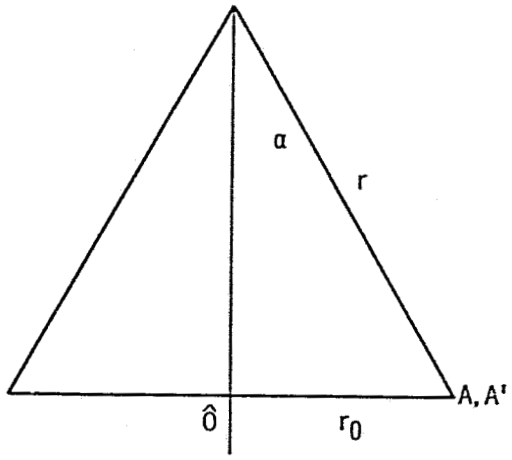

Figure 3. - Cone formed from the disk of figure.

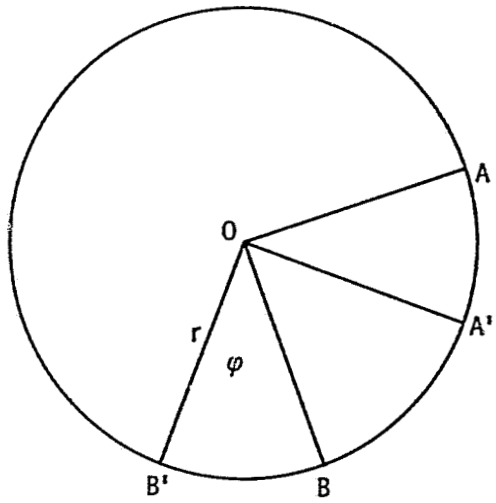

(a) CUT OUT DISK.

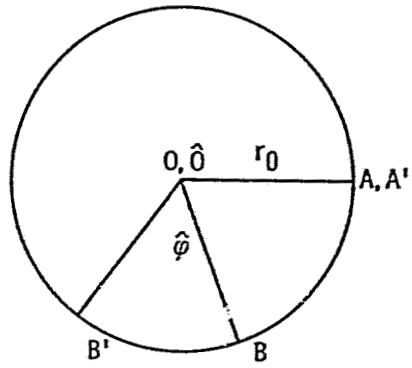

(b) TOP VIEW OF THE CONE.

Figure 4. - Disk with cut out section and top view of resulting cone.

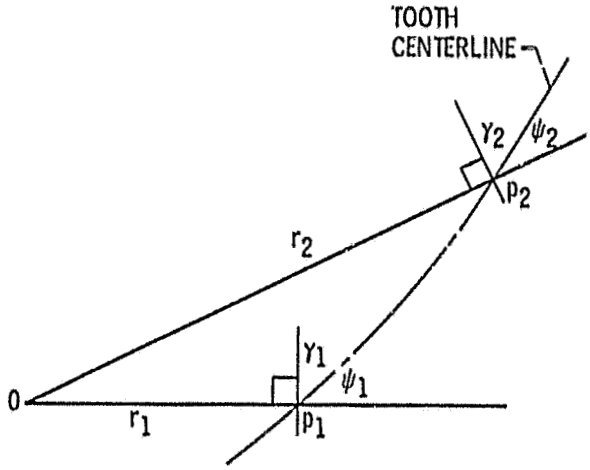

Figure 5. - Radial inclination of the tooth centerline.

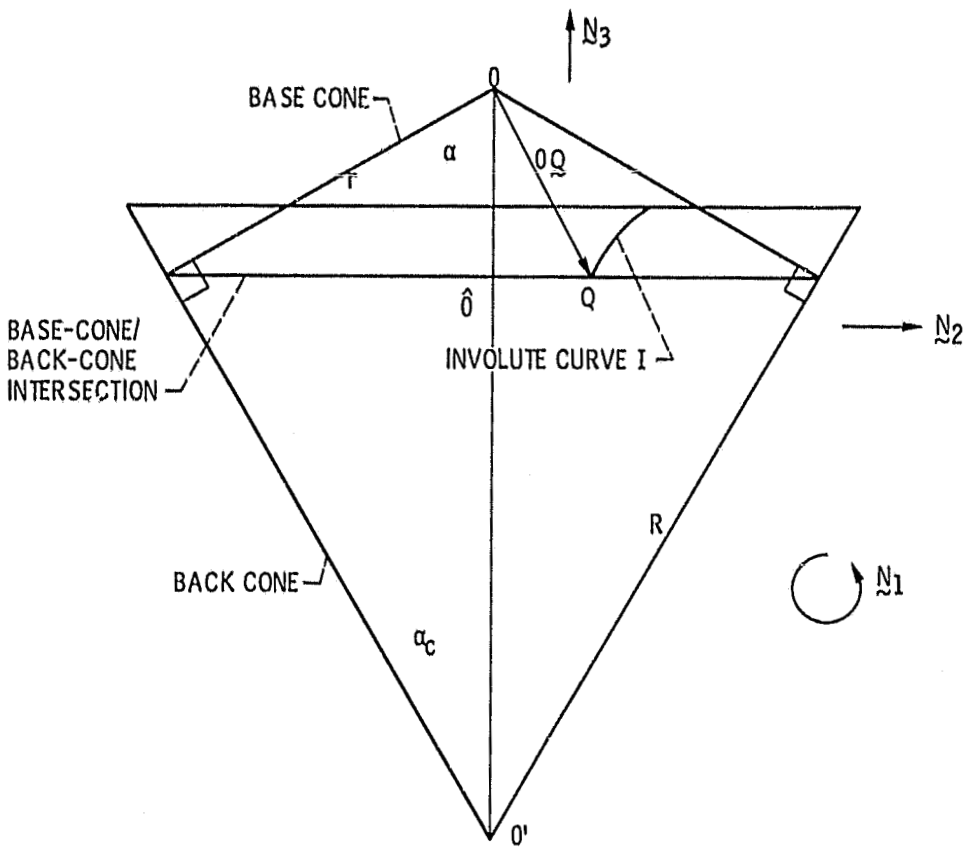

Figure 6. - Base cone and involute spindling around a back cone.

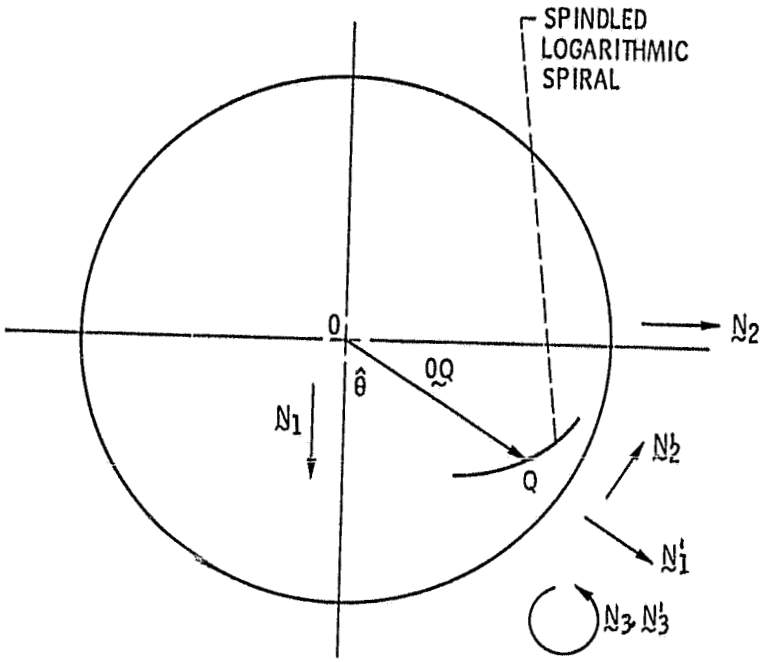

Figure 7. - Top view of base-cone/back-cone intersection and projected curve of a typical tooth.

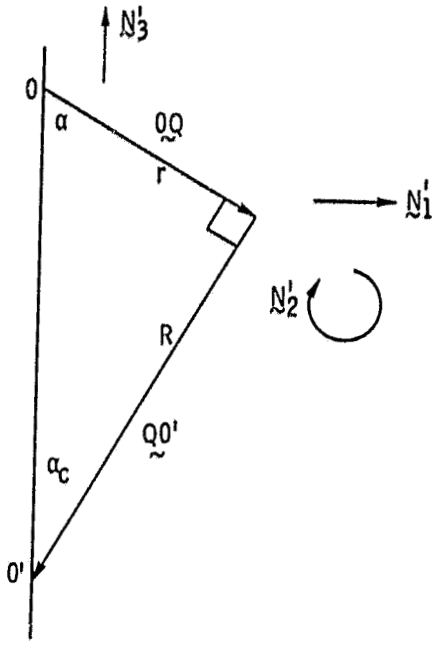

Figure 8. - True view of vectors $\underset{\sim}{0Q}$ and $\underset{\sim}{Q0'}$.

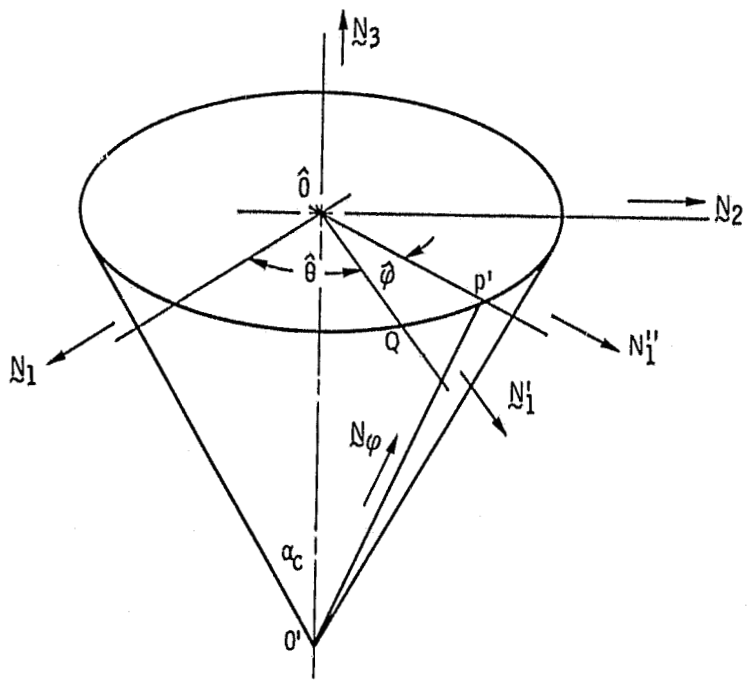

Figure 9. - Back cone unit vectors.